
Article:
Akinola, T.E., Oko, E. and Wang, M. (2019) Study of CO2 removal in natural gas process using mixture of ionic liquid and MEA through process simulation. Fuel, 236. pp. 135-146. ISSN: 0016-2361

https://doi.org/10.1016/j.fuel.2018.08.152

Study of CO_2 removal in natural gas process using mixture of ionic liquid and MEA through process simulation

Toluleke Emmanuel Akinola, Eni Oko, Meihong Wang*,*
Department of Chemical and Biological Engineering, University of Sheffield S1 3JD
*Corresponding Author. Tel.: +44 114 222 7160. E-mail address: Meihong.Wang@sheffield.ac.uk

Abstract

There has been a shift to less carbon intensive fuels such as natural gas to meet energy demand due to increasing pressure to cut CO_2 emissions. This has prompted a need to assess unconventional and contaminated natural gas reserves (which contains CO_2 concentration of 20mol% or more). The CO_2 capture process with MEA as the solvent is mostly adopted to treat contaminated natural gas. In this study, the option of using a blend of ionic liquids (IL) and MEA as a promising solvent in the process was investigated through modelling and simulation. A detailed rate-based model was developed for both MEA (30wt%) solvent and IL (30wt%)-MEA (30wt%) blend using Aspen Plus® to assess both process and economic performances. The 1-Butylpyridinium ([bpy][BF_4]) ionic liquid was selected in this study. The physiochemical properties of [bpy][BF_4], predicted using Aspen Plus®, showed good accuracy compared with experimental data. The results from this study showed about 15% and 7.44% lower energy consumption in the reboiler duty and CO_2 removal cost respectively with aqueous [bpy][BF_4]-MEA solvent compared to 30 wt% MEA solvent. It is concluded that the aqueous [bpy][BF_4]-MEA solvent is therefore a promising solvent that could replace 30 wt% MEA solvent in this process.

Keywords*: Natural gas processing, CO_2 removal, Chemical absorption, MEA, Ionic liquid, Process simulation*

Abbreviations

ACC	Annual Capital Cost
AOC	Annual Operating Cost
[bpy][BF_4]	1-butylpyridinium tetrafluroborate
[bheaa]	Bis(2-hydroxyethyl) ammonium acetate
[bmim][BF_4]	1-butyl-3-methylimidazolium tetrafluoroborate
[bmim][DCA]	1-butyl-3-methylimidazolium dicyanamide
CW	Cooling Water
DEA	Diethanolamine
DHVLB	Heat of Vaporization at T_b
D&M	Distribution and Marketing
Elec	Electricity
ENRTL	Electrolyte Non-Random Two Liquid
FC-CS	The Fragment contribution – corresponding states
FOC	Fixed Operating Cost
IL	Ionic Liquid
IEA	International Energy Agency
LNG	Liquefied Natural Gas

MDEA	Methyldiethanolamine
MEA	Monoethanolamine
Mis	Miscellaneous
R&D	Research and Development
RK	Redlich Kwong
RKTZRA	Rackett /Campbell-Thodos Mixture Liquid Volume
RTILs	Room temperature ionic liquids
TSILs	Task specific ionic liquids
V_B	Liquid Molar Volume at Tb
VOC	Variable operating cost
VLSTD	Standard liquid Volume

23

Nomenclature

$C_{1i} - C_{3i}$	Equation coefficients for (7)
$C'_{1i} - C'_{3i}$	Equation coefficients for (8)
Z_i^{*RA} and d_i	Equation coefficients for (9)
$A_i - C_i$	Equation coefficients for (10)
$C''_{1i} - C''_{5i}$	Equation coefficients for (11)
$D_i - D_{iii}$	Equation coefficients for (12)
H_{ij}	Henry Constant
P_i^v	Vapour pressure of component i, Pa
P_c	Critical pressure, bar
Q_{reb}	Reboiler duty, kJ/kg_{co2}
Q_{cond}	Condenser duty, kJ/kg_{co2}
Q_{cooler}	Cooler duty, kJ/kg_{co2}
T	Temperature, K
T_b	Normal Boiling temperature, K
T_c	Critical temperature, K
T_r	Reduced temperature, K
V_c	Critical Volume, cc/mol
W_{pump}	Pump power kJ/kg_{co2}
Z_c	Critical Compressibility factor
σ_i	Surface tension, mN/m

η_i	Liquid Viscosity, cP
ρ_i	Liquid molar density, mol/cc
Ω	Omega
ΔH_f^0	Standard heat of formation, kJ/mol
ΔH_c^0	Standard heat of combustion, kJ/mol
λ_i	Thermal conductivity, kcal-m/hr-m^2-K

1. Introduction

1.1 Background

The need to reduce emissions has favoured a shift towards low carbon fuels such as natural gas for energy generation [1]. it is predicted that a switch to low carbon fuels will contribute about 15% in expected CO_2 emission cuts by 2050 [2]. Globally, mineable natural gas reserves are far smaller in comparison to that of carbon intensive fuels (*i.e.* coal) and as such, natural gas supply is less secured and expensive. This has prompted the need to re-assess the development of unconventional, stranded, contaminated and sour natural gas reserves [3]. However, raw natural gas is known to contain acid gas such as CO_2 with concentration of about 20mol% and more, which makes these reserves economically unviable. These natural gas reserves are predominantly in SE Asia, NW Australia, Central USA, North Africa and the Middle East [4]. These locations are far from the established gas markets in Western Europe, Japan and South Korea. Thus, a large amount of natural gas must be conveyed either via long distance pipeline or as Liquefied Natural Gas (LNG) [3]. The presence of CO_2 in natural gas limits its quality (heating value) and the liquefaction process performance.

Natural gas sweetening technologies are adopted to remove CO_2, so natural gas can meet acceptable standards for pipeline transport to end-users and/or liquefaction process for LNG [5]. Natural gas sweetening process involves CO_2 separation from the gas mixture using techniques such as physical absorption, chemical absorption, adsorption, cryogenic separation and membrane separation among others [5]. Chemical absorption is the most commonly and widely used separation method in natural gas sweetening processes [6, 7]. However, it is expensive especially due to the high energy penalty of the process [8]. Thus, there is a need to explore different options for reducing the high-energy penalty of the process.

1.2 Motivation

Amine-based CO_2 absorption/desorption process has been in use for decades in the industry for CO_2 removal from gas mixtures such as natural gas among others [3, 6, 9, 10]. This is primarily due to its relatively rapid kinetics of the amine solvents [3, 6]. However, amine solvents generally require high energy for regeneration. They also tend to stimulate equipment corrosion and degrade rapidly during operation. This makes the operating cost for amine-based process generally high [6]. Thus, attention has shifted to development of new solvents that have less energy requirement for regeneration and are

more stable, with less tendency to degrade and lower potential for stimulating corrosion. One of such solvents is ionic liquids (ILs).

Ionic liquids (ILs) are generally classified as compound composed entirely of ions (cations and anions). They tend to be liquids over a wide range of temperature and are non-volatile which makes them good solvents for a variety of materials. The tunability capability of the ionic liquid makes it possible to tune the ionic liquid structure to suit a specific process requirement by altering either the cation or anion. Some of the commonly encountered cations and anions are shown in Fig.1. ILs requires less energy for regeneration and are environmentally friendly solvents [5]. In addition, they are thermally stable and have low vapour pressure among others. These qualities satisfy the requirements of a more energy-efficient solvent for CO_2 absorption/desorption process than amine solvents [5, 11].

Several studies on the properties and application of various ILs for natural gas sweetening and carbon capture through experimental investigations have been carried out [11-18]. From these investigations, it was concluded that the use of ILs only as a solvent is less competitive when compared with MEA. This is due to its low CO_2 absorption capacity. In the quest to find a more competitive solvent, attention has been given to functionalized ILs, supported IL membranes and polymerized ILs [5]. These ILs formulation are considered more expensive than the traditional amine solvents [5]. Also, gas-liquid mass transfer rates are low with ILs due to their high viscosities, resulting in a low reaction rate with CO_2, making them less competitive than amine solvents [5]. These reasons have made IL solvents currently not industrially viable for CO_2 absorption/stripping processes in a large scale [5]. On the other hand, the option of blending ILs and amine solvents have shown a lot of promise [3, 5, 20]. This basically involves merging an eco-friendly IL with the high binding capacity amines [5]. It has been shown that this option requires less regeneration energy than conventional amine process, better process economics and substantially higher gas-liquid mass transfer rates than only ILs [11].

1.3 Previous studies

Use of IL-Amine blends for natural gas sweetening and carbon capture is driven by the need to develop new solvents with a CO_2 loading capacity comparable to the amine-based solvents and with great reduction in the energy required for regeneration [11]. The section gives a review on the application of IL-amine blends for natural gas sweetening and carbon capture.

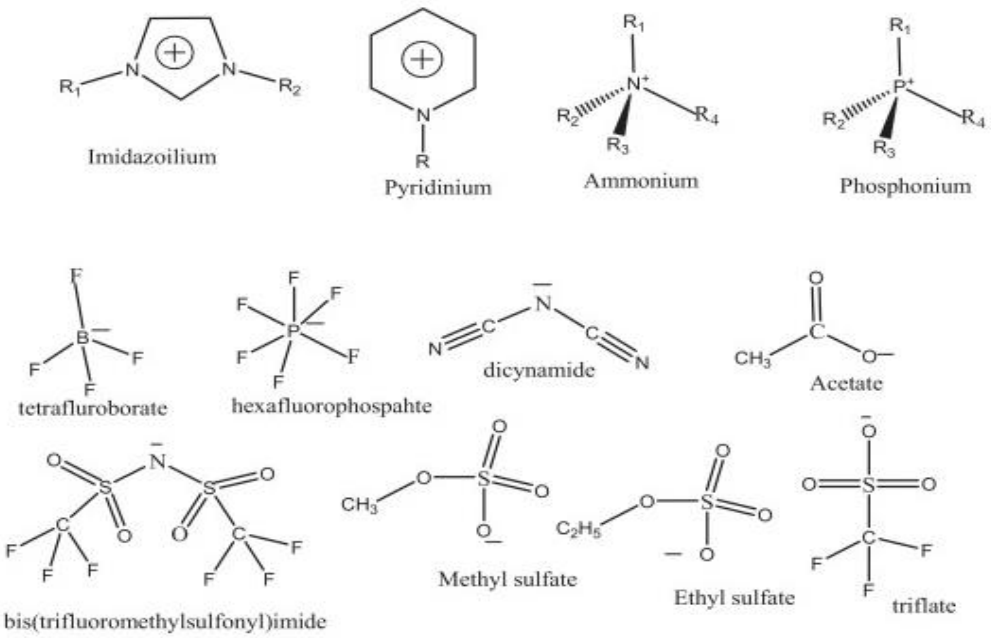

Fig. 1 General Structure of various cations and anions used for Ionic liquid formulation [5]

Various researchers have carried out experimental investigations on the physical properties and absorption capacity of IL-amine blend. Investigation by Camper et al.[20] on the solubility of CO_2 in IL-amine blend revealed that the RTIL-amine (RTIL-MEA and RTIL-DEA) blends demonstrated rapid and reversible CO_2 capture performance, while the amine functionalised TSIL exhibited a slower CO_2 capture performance due to its high viscosity. Similar investigation carried out by Feng et al.[21] showed that temperature increase enhances the absorption rate. The influence of temperature on the absorption rate is said to diminish after a long period.

study on CO_2 solubility using two ILs blended with MEA ([bheaa]-MEA and [bmim][BF_4]-MEA) by Taib and Murugesan [22] demonstrated that CO_2 solubility in MEA exhibit chemical solubility while the solubility of CO_2 in IL exhibits physical solubility, indicating that the CO_2 removal mechanism can both be physiosorption and chemisorption [23]. Further details on the mechanism analysis for both solvents can be seen in Taib and Murugesan [22].

Experiment studies on CO_2 solubility and physical properties of IL-amine mixture highlighted the impact of H_2O and amine on the physical properties of the absorbents (particularly density and viscosity), which enhances CO_2 capture performance [24, 25]. The CO_2 absorption capacity of the IL-amine blend was mainly a function of amine concentration and the presence of water reduces the IL-amine blend viscosity, which makes it an industrially viable solvent [24]

Further experimental investigation on IL-amine solvent revealed that the hybrid solvent achieved lower energy consumption compared to conventional solvent [26] and demonstrated better corrosion control with carbon steel material compared with aqueous amine[27]. More experimental studies on IL-amine

solvents can be found in [28-31]. It can be seen that an industrially competitive hybrid solvent could be developed by blending ILs with amine solutions to enhance the CO_2 removal performance.

Studies involving whole process analysis of CO_2 removal from gas mixtures using IL-based solvents have also been reported [11, 26]. Despite the successful experimental investigations on the application of IL-amine blends for CO_2 removal, there have been little research on modelling and simulation of the natural gas sweetening process/ carbon capture process using the hybrid solvent to our knowledge. It is necessary that the thermodynamic model adopted accurately predict the hybrid solvent behaviour. This will ensure accurate configuration and operation selection [5]. Huang et al.[32] predicted the critical properties of various IL using the FC-CS method and then carried out thermodynamic modelling, process simulation and cost estimation of CO_2 removal (absorption) process from flue gas (6.37mol% CO_2, 69.46mol%N_2, 3.66mol% O_2, 20.51mol% H_2O) [11]. In the study, three (3) ILs ([bmim][BF_4], [bmim][DCA] and [bpy][BF_4] blended with aqueous MEA solution were investigated. The physicochemical properties of the ILs were predicted by various temperature-dependent correlations. The phase equilibria were modelled based on the Henry's law and NRTL equation. The values calculated agree well with experimental solubility data from literature. From the process simulation assessment, the [bpy][BF_4] –MEA hybrid solvent (with 30wt% IL and 30wt% MEA) process gave savings of 15% and 11% regeneration duty and capture cost compared to the reference MEA based process. Other studies on process analysis of gas mixtures using IL-based solvents includes [33, 34].

1.4 Aim and Novelty

The aim of this study is to analyse CO_2 removal from raw natural gas in the context of natural gas sweetening using [bpy][BF_4]-MEA mixture through modelling and simulation. [bpy][BF_4] is selected mainly due to its low cost [19] and low toxicity [35] compared to the imidazolium-based ionic liquids which has been experimentally investigated successfully for removal of CO_2.

In carrying out this study, we intend to carry out an energy and cost performance analysis for the IL-MEA process in comparison to the MEA only process. Ionic liquid-amine blends have been reported for CO_2 removal from power plant flue gases by Huang at al. [11]. However, CO_2 removal from natural gas presents a unique scenario involving higher operating pressure (up to 69 bar) and a mixture of light hydrocarbons, namely methane, ethane, propane etc. This will affect the thermodynamics of the process and mass transfer performance and possibly lead to results that are dissimilar to Huang et al. [11]. Thus, it is necessary that a study dedicated to CO_2 removal from natural gas be carried out in the quest to discover a more energy efficient solvent to replace the amine based solvent. Physical properties of the IL in this study were obtained from experimental data available in [13, 15, 17, 36].

2. Process benchmark

2.1 Description

The process schematic for sour natural gas production and processing is shown in Fig.2. In this process, sour gas coming from the production well flows through a separator to knock out condensates in the gas before entering the sweetening process, which is of interest in this study (Fig.3).

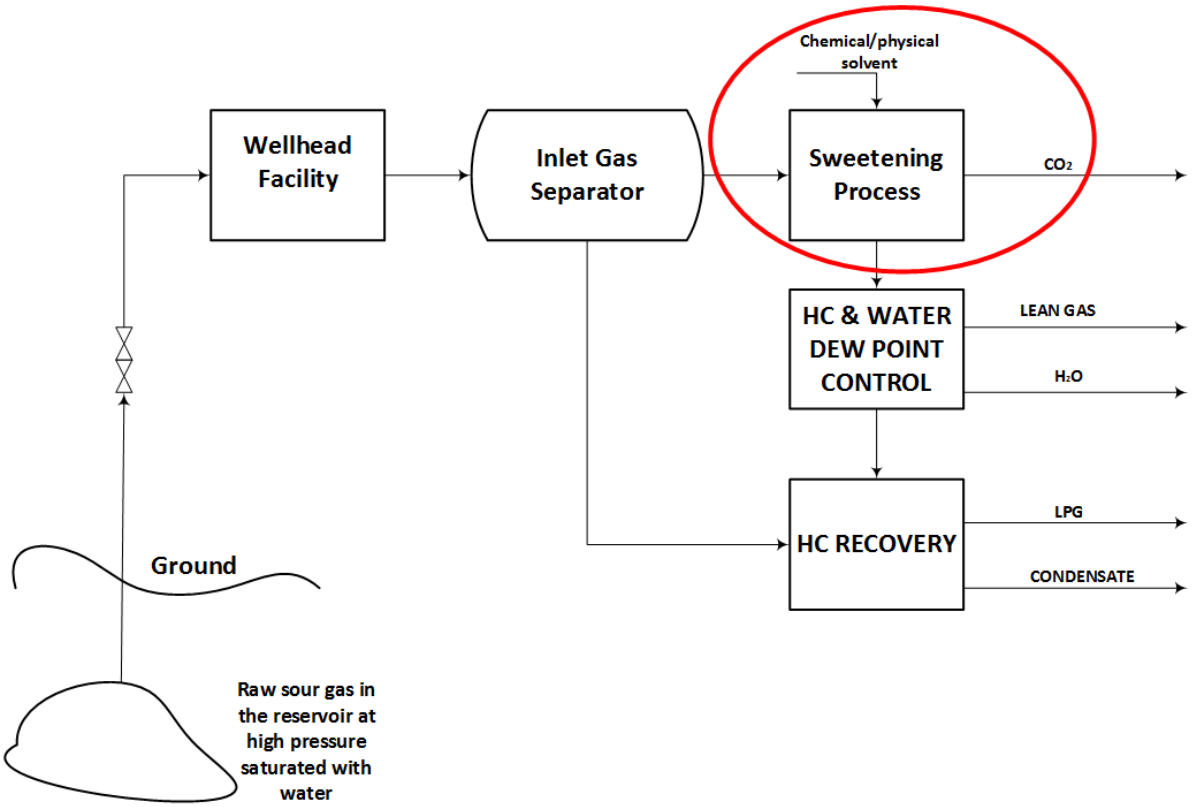

Fig. 2 Schematic diagram of sour natural gas production/processing [37]

The Natural gas sweetening process mainly consists of absorption and regeneration columns (See Fig.3). Sour gas (Table 1) flows in the absorber, from the bottom stage. The lean solvent absorbs CO_2 from the sour gas by forming weakly-bonded compounds while flowing in a counter-current manner. The treated gas exits from the top of the absorber while the CO_2 rich solvent exits from bottom [6, 38]. The rich solvent leaving the absorber, flows to the flash drum to remove absorbed hydrocarbons. The rich solvent leaves the flash drum to the rich/lean exchanger, where heat is absorbed from the lean solution. The heated rich solvent flows to the stripper where CO_2 is recovered from the solvent through heat input to the reboiler. The lean solvent is recycled to the absorber as it flows from the regeneration column bottom through the rich/lean exchanger, cooler and pump. The process flow diagram shown in Fig. 3 is adopted for both MEA and hybrid solvent based process.

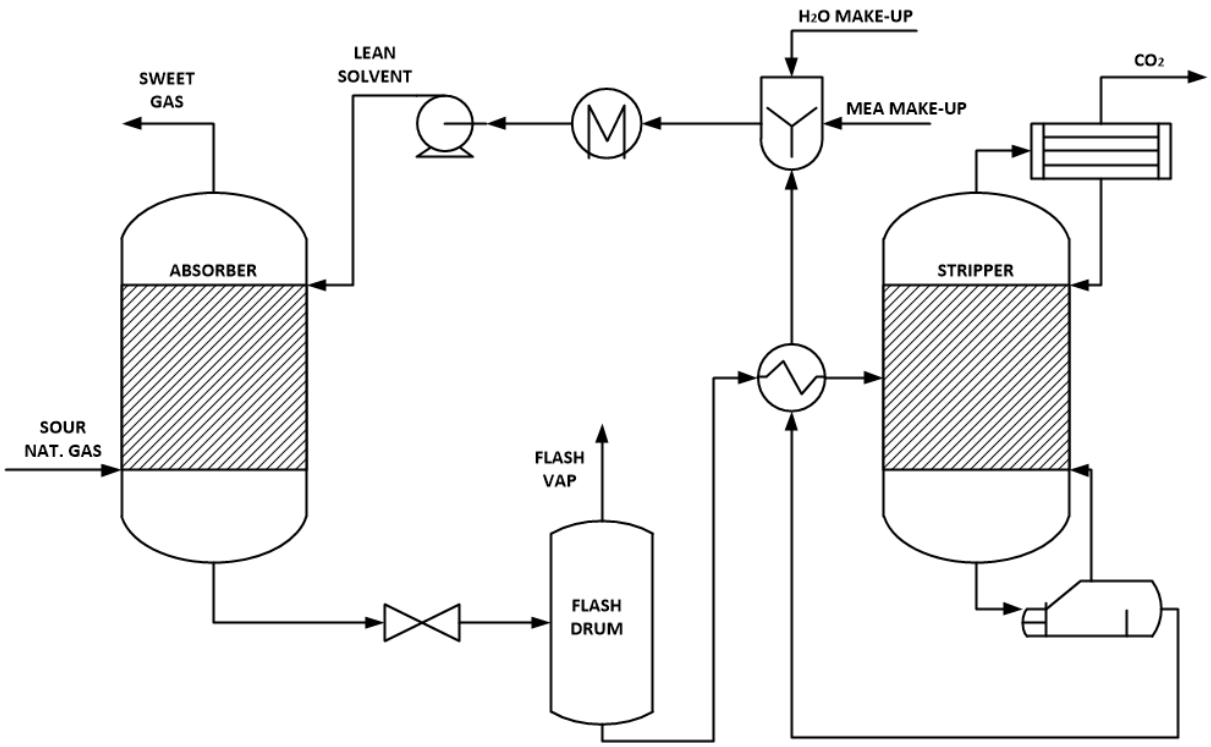

Fig. 3 CO_2 removal process Flow diagram [9]

3. Methodology

3.1 Model Development

The absorber and stripper model were developed using RADFRAC model in Aspen Plus®. RADFRAC supports both equilibrium-based and rate-based approaches for mass transfer modelling. Models based on both approaches were developed in this study. In the equilibrium-based model, the liquid and gas phases are assumed to be in equilibrium [39]. On this basis, heat and mass transfer calculations are then based on estimated efficiency parameters. The rate-based model on the other hand includes detailed mass transfer calculations based on the two-film theory (Fig.4). The following assumptions were made during the model development [39]:

- Mixed flow regime
- Negligible heat loss to the surroundings
- N_2 and hydrocarbon not readily soluble in IL and MEA
- Chemical reactions are completed in the liquid film only

Table 1 Sour Gas Conditions (Obtained from HYSYS [40] with modifications)

Parameters	**Unit**	**Value**
Temperature	˚C	35
Pressure	bar	69
Flowrate	MMSCFD (Million Standard cubic feet per day)	25
Component		
Nitrogen	mol%	0.16
Water	mol%	1.22
Methane	mol%	73.76

Parameters	Unit	Value
Ethane	mol%	3.93
Propane	mol%	0.93
Carbon dioxide	mol%	20.00

171

172
173
174

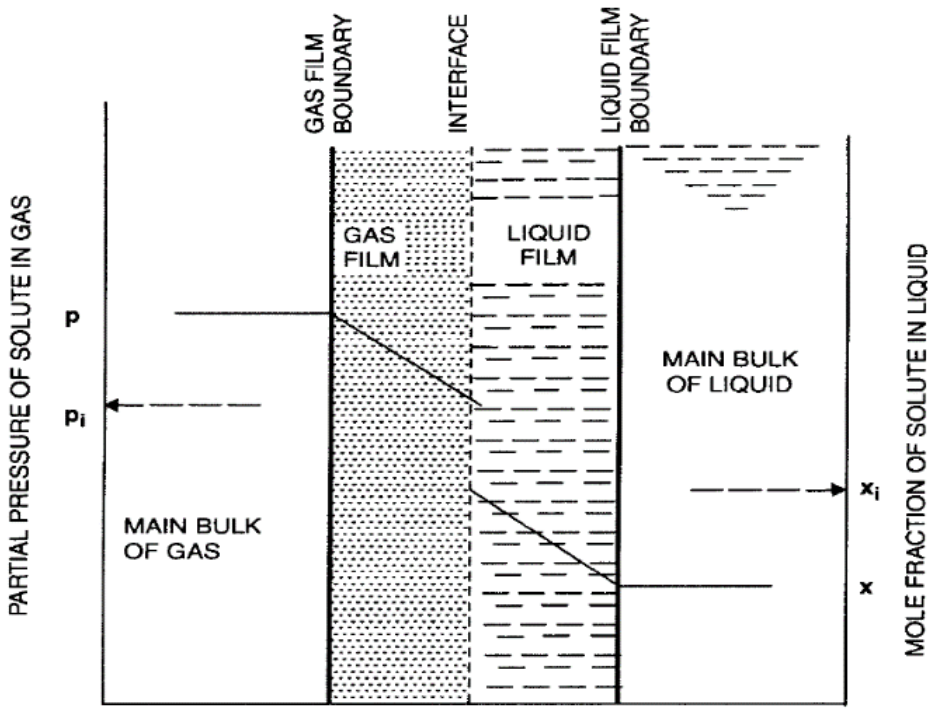

175
176 **Fig. 4 Two-Film Theory [41]**

177

178 3.2 Thermodynamic model

179 3.2.1 CO_2 removal process with MEA

180 Thermodynamic modelling of the conventional CO_2 removal process that involves physicochemical
181 properties, phase equilibrium and chemical reactions of the component system was carried out using
182 the Electrolyte Non-Random Two Liquid model (ELECNRTL). The ELECNRTL model is commonly used
183 for thermodynamic modelling of MEA scrubbing process [11, 39, 42] and has been verified through
184 industrial applications. The following are the set of chemical reactions considered for the system [6, 9].

$$2H_2O \rightleftharpoons H_3O^+ + OH^+ \quad (1)$$

$$H_2O + HCO_3^- \rightleftharpoons H_3O^+ + CO_3^{-2} \quad (2)$$

$$H_2O + MEA^+ \rightleftharpoons H_3O^+ + MEA \quad (3)$$

$$H_2O + MEACOO^- \rightleftharpoons MEA + HCO_3^- \quad (4)$$

$$CO_2 + 2H_2O \rightleftharpoons HCO_3^+ + HCO_3^- \quad (5)$$

185

186 Temperature dependent correlations are used for estimating equilibrium constants as follows:

$$\ln k_j = A + \frac{B}{T} + C\ln T + DT \quad (6)$$

The reaction equilibrium constants as well as physiochemical properties (both scalar and temperature dependent) of each component, binary parameters and electrolyte pairs were retrieved from the Aspen properties databank.

3.2.2 CO_2 removal process using [bpy][BF_4]-MEA

3.2.2.1 Physicochemical properties

The properties of MEA are available in ASPEN properties databank as previously described. However, there is little information on pyridinium based ionic liquid properties in the databank. Thus, the properties of [bpy][BF_4] were obtained from literature. The scalar properties of [bpy][BF_4] such as the properties were obtained from literature (Table 2). Aspen Plus simulation software was used to estimate other relevant scalar properties of [bpy][BF_4].

Table 2 Scalar properties of [bpy][BF_4] [17, 32]

Parameters	Unit	Value
T_b	K	697.9
P_c	bar	25.8
ΔH_f^0	kJ/mol	-1356.3
ΔH_c^0	kJ/mol	-5451

Temperature dependent properties of [bpy][BF_4] such as heat capacity, molar volume, surface tension, thermal conductivity were obtained using the following equations [11]:

Vapour pressure $$\ln P_i^v = C_{1i} + \frac{C_{2i}}{T + C_{3i}} \quad (7)$$

Heat capacity $$C_{pi} = C'_{1i} + C'_{2i}T + C'_{3i}T^2 \quad (8)$$

Molar Volume $$V_m^l = \frac{RT_{ci}[Z_i^{*,RA}(1 + d_i(1 - T_r)]^{[1+(1-T_r)^{\frac{2}{7}}]}}{P_{ci}} \quad (9)$$

Viscosity $$\ln \eta_i = A_i + {}^{B_i}/_{T} + C_i \ln T \quad (10)$$

Surface tension $$\sigma_i = C''_{1i}(1 - T/T_{ci})^{(C''_{2i}+C''_{3i}T_{ri}+C''_{4i}T_{ri}^2+C''_{5i}T_{ri}^3)} \quad (11)$$

Thermal conductivity $$\lambda_i = D_i + D_{ii}T + D_{iii}T^2 \quad (12)$$

The Liquid heat capacity is a basic thermodynamic property used for specifying the amount of heat needed to change a liquid temperature by a given amount while the molar volume is a transport property used to describe the volume occupied by one mole of the component at a given temperature and pressure. Given that ionic liquids are well known as a non-volatile liquid whose vapour pressure is difficult to observe [11].Equation coefficients for (8) to (12) were estimated using data obtained from literature [13, 15, 17, 36] on Aspen Plus® simulation software.

3.2.2.2 Phase Equilibria Modelling

Generally, the phase equilibrium of the CO_2-H_2O-[bpy][BF_4]-MEA system was based on ELECNRTL model. The electrolyte and interaction parameters of MEA and other components are available in

ASPEN properties databank except the pyridinium based IL. The solubility of N_2 in [bpy][BF_4] was neglected [43]. The phase equilibrium relationship for CO_2 – [bpy][BF_4] system was modelled as follows:

$$\varphi_i^V y_i P = x_i \gamma_i^* H_{ij} \quad \textbf{13}$$

$$\gamma_i^* = \left(\frac{\gamma_i}{\gamma_i^\infty}\right) \quad \textbf{14}$$

where γ_i^∞ is the infinite dilution activity coefficient of component i in the mixture. Due to the low vapour pressure of ILs, it is assumed that there will be no IL in the gaseous phase thus, the Henry's law constant of component i is defined as:

$$H_{ij} = \frac{\varphi_i^v P}{x_i \gamma_i^*} \quad \textbf{15}$$

where $H_{ij}, P, x_i, \gamma_i^*$ and φ_i^V are Henry constant, total pressure, mole fraction of component i in liquid phase, activity coefficient of component i in liquid phase and the fugacity coefficient in the vapour phase respectively. Redlich-Kwong (R-K) equation of state was used to obtain the fugacity coefficient in vapour phase as follows:

$$ln\varphi = Z - 1 - \ln(Z - bp/RT) - \left(\frac{a/R^2T^{2.5}}{b/RT}\right)\ln(1 + bp/ZRT) \quad \textbf{16}$$

$$Z = pV/RT \quad \textbf{17}$$

$$p = \frac{RT}{V-b} - \frac{a}{T^{0.5}V(V+b)} \quad \textbf{18}$$

$$a = 0.42748\frac{R^2T_c^{2.5}}{P_c} \quad \textbf{19}$$

$$b = 0.08664\frac{RT_c}{P_c} \quad \textbf{20}$$

where φ is the fugacity coefficient, Z is the compressibility factor, R is the gas constant, a and b are equation of state constants. T_c, P_c, V are the Critical temperature, critical pressure and molar volume respectively. The Henry's constants of component i in mixture j were obtained by using the temperature dependent henry constants equation shown below [11]:

$$\ln H_{ij} = a_{ij} + b_{ij}/T + c_{ij}\ln T + d_{ij}T \quad \textbf{21}$$

where a_{ij} – d_{ij} are the Henry constant binary interaction parameters. The liquid activity coefficient of CO_2 in the mixture was modelled by the NRTL using (22):

$$\ln Y_i = \frac{\sum_{j=1}^{\delta} x_j x_{ji} G_{ji}}{\sum_{i=1}^{\delta} x_k G_{ki}} + \sum_{j=1}^{\delta}\left(\frac{x_j G_{ij}}{\sum_{k=1}^{\delta} x_k G_{kj}}\left(\tau_{ij} - \frac{\sum_{m=1}^{\delta} x_m \tau_{mj} G_{mj}}{\sum_{k=1}^{\delta} x_k G_{kj}}\right)\right) \quad \textbf{22}$$

$$G_{ij} = \exp(-\alpha_{ij}\tau_{ij})$$

$$\tau_{ij} = a_{ij} + {}^{b_{ij}}/_{T} + e_{ij}\ln T + f_{ij}T$$

$$\alpha_{ij} = c_{ij} + d_{ij}(T - 273.15)$$

$$\tau_{ii} = 0;\ G_{ii} = 1;\ c_{ij} = 0.3$$

where a_{ij}, b_{ij}, c_{ij}, d_{ij}, e_{ij} and f_{ij} are the binary interaction parameter, δ is the number of components and x is the mole fraction. The parameters of Henry constants and NRTL binary interaction parameters between CO_2 and [bpy][BF_4] generated by Huang et al. [11] were inputted in ASPEN Plus® simulation software. The parameters have been validated in Huang et al. [11].

For the H_2O-[bpy][BF_4]-MEA system, VLE calculation was carried out based on the modified Raoult's law as follows:

$$y_i p = x_i \gamma_i p_i^v \quad \textbf{23}$$

Based on the assumption that the vapour mole fraction of [bpy][BF_4] is negligible, (23) is simplified into the following equations for both H_2O-[bpy][BF_4] and H_2O-[bpy][BF_4]-MEA;

$$p = x_a \gamma_a p_a^v \quad \textbf{24}$$

$$p = x_a \gamma_a p_a^v + x_c \gamma_c p_c^v \quad \textbf{25}$$

where subscripts "a" and "c" denotes H_2O and MEA respectively. [9] obtained the binary parameters of [bpy][BF_4]-H_2O and [bpy][BF_4]-MEA system from experimental data based on (24) and (25) in combination with NRTL model (22). These binary parameters obtained were used in this study.

3.3 Process Simulation

Acid gas sweetening process models using aqueous MEA solvent and aqueous [bpy][BF_4]-MEA solvent were developed in Aspen Plus®. The composition of the solvents for each process are shown in Table 3. The Equilibrium based approach was basically adopted to estimate the column sizes. Under rate based approach, Bravo et al.[44] correlation was used to estimate the mass transfer coefficient and Interfacial area while the Chilton and Colburn correlation was used to estimate the heat transfer coefficients. Equipment specifications used in the process simulation are detailed in Table 4. The model topology is given in Fig.5.

Both process models were simulated to achieve 1 mol% of CO_2 at the absorber gas outlet and 95 wt% CO_2 concentration recovered from the stripper by manipulating the lean solvent flowrate and reflux ratio.

Table 3 Components and composition

MEA		
H_2O	wt%	70
MEA	wt%	30
IL-MEA		
H_2O	wt%	40
MEA	wt%	30
[Bpy][BF_4]	wt%	30

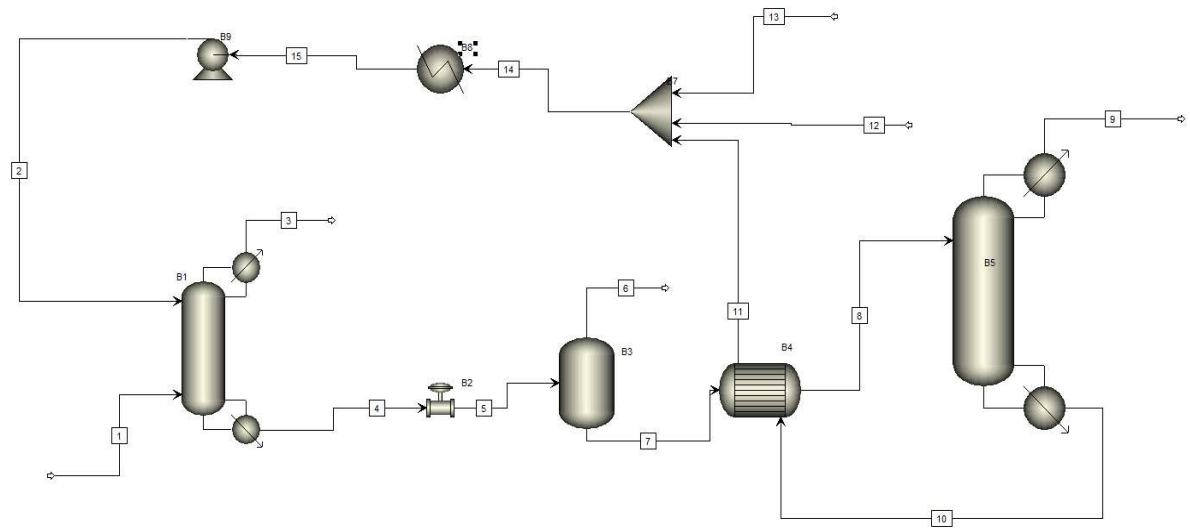

248

249 **Fig. 5 Process model topology in ASPEN Plus®**

250

251 **Table 4 Base specifications of each Unit Operation**

Unit Operation Specification		**Unit**
Absorber		
Theoretical stages number	20	
Column height	6	meter
Top stage Pressure	6860	kPa
Packing Type	FLEXIPAC	
Packing dimension	250Y	
Packing material	Metal	
Flash tank		
Pressure	620	kPa
Heat Exchanger		
Hot/Cold outlet temperature approach	5	˚C
Hot side pressure drop	0	kPa
Stripper		
Number of stages	20	
Condenser	Partial-vapour	
Top stage pressure	170	kPa
Column pressure drop	0.1	kPa
Column height	6	meter
Packing Type	FLEXIPAC	
Packing dimension	250Y	
Packing material	Metal	
Cooler		

Unit Operation Specification		**Unit**
Temperature	38	˚C
Pump		
Discharge pressure	6860	kPa

252

253 3.3.1 Energy performance

254 The specific (reboiler) heat duty is a critical parameter to measure performance in the CO_2 removal
255 process. The specific heat duty measures heat required in the reboiler to remove 1tonne of CO_2. In this
256 study, the energy consumption from the energy utilizing equipment (pump and reboiler) were
257 considered to measure the energy performance of both MEA and [Bpy][BF_4]-MEA based process. For
258 the reboiler, it is assumed that steam is supplied from the steam boiler at a pressure of 3 bar to achieve
259 reboiler temperature specification (120^{o}C).

260 3.3.2 Cost Analysis

261 The cost of CO_2 removed for both process, which depends on the annual capital and operational cost,
262 was estimated based on the breakdown adopted in [11, 45]. The equipment size selection and costing
263 was carried out using Aspen Process Economic analyzer software, based on the first quarter of 2013
264 chemical engineering plant cost index (CEPCI). The annual capital cost (ACC) is calculated as:

$$\mathrm{ACC} = \frac{\mathrm{TCC}}{((1+r)^n - 1)/r\,(1+r)^n} \qquad \textbf{26}$$

265 where TCC is the total capital cost with an interest rate (r) and project lifetime (n) of 20% and 30years
266 respectively. A breakdown of the total capital and operational cost (fixed and variable cost) components
267 following [11, 45, 46] is detailed in Table 5. The cost of MEA and pyridinium based ionic liquid solvents
268 adopted for this study was 0.93 GBP/kg (1.25 USD/kg) and 4.88 GBP/kg (6.6 USD/kg) respectively [11,
269 47].

270 **Table 5 Cost Estimation Breakdown**

Capital Cost Breakdown	**(%) of Equipment Cost (EC)**
Installed Cost	10% of EC
Instrumentation and Control	20% of EC
Piping	30% of EC
Electrical	5% of EC
Building and building Services	10% of EC
Yard Improvements	10% of EC
Land	5% of EC
Miscellaneous	2% of EC
Direct Cost (DC)	**Sum of the above**
Engineering and Supervision (E&S)	15% of DC
Contingency (C)	11% of DC

Procurement Cost (PC)	2% of DC
Indirect Cost (IDC)	**E&S + C + PC**
Fixed Capital Cost (FCC)	DC + IDC
Working Capital (WC)	15% of FCC
Start-up Cost (SC)	1% of FCC
Initial Solvent Cost (ISC)	Solvent circulation x cost
TCC	**FCC + WC + SC + ISC**
Operating Cost Breakdown	
Steam Utility Cost (£/GJ)	1.63
Cooling water Utility Cost (£/GJ)	0.157
Electricity Utility Cost (£/kWhr)	0.057
Make-up water Cost (£/kg)	0.00037
Make-up MEA Cost (£/kg)	0.925
Make-up IL Cost (£/kg)	4.884
Miscellaneous operating cost	2% of VOC
VOC	**Sum of the above cost**
FOC	**Sum of the below cost**
Local Tax (LT)	1% of FCC
Insurance	1% of FCC
Maintenance (M)	3% of FCC
Operating Labour (OL)	£ 26.64 per hr
Lab Costs	20% of OL
Supervision	20% of OL
Plant Overheads	50% of OL
Operating Supplies	15% of M
Admin Cost	15% of OL
Distribution and Marketing	0.5% of OC
R&D Cost	5% of OC
Operating Cost (OC)	**VOC + FOC**

3.3.3 Process Analysis

Analysis on the impact of pyridinium based ionic liquid concentration on the energy and cost performance of hybrid solvent-based process was carried out. The mass fraction of [bpy][BF_4] in the hybrid solvent was varied while keeping the mass fraction of MEA constant. For each case considered, the process was simulated to achieve 1 mol% of CO_2 at the absorber gas outlet and 95 wt% CO_2 concentration recovered from the stripper at minimum energy consumption.

4. Physiochemical Property Validation of [bpy][BF_4]

Scalar properties and the coefficients of temperature dependent properties of [bpy][BF_4] estimated using Aspen Plus® simulation software are listed in Tables 6 and 7. The temperature dependent properties estimated by Aspen Plus® gave a good prediction when compared with the experimental data retrieved from literature as shown in Fig.6.

Table 6 Scalar Property Parameters of [bpy][BF_4]

T_C	℃	723.81
DHVLB	J/kmol	6.54E+07
V_B	m^3/kmol	0.23
RKTZRA		0.22
VLSTD	m^3/kmol	0.18
V_C	m^3/kmol	0.82
Z_C		0.26
P_C	bar	25.8

Table 7 Temperature dependent parameter for [bpy][BF_4]

Liquid Viscosity (N-sec/m^2)	
A_i	-2.435E+03
B_i	1.618E+05
C_i	3.380E+02
Liquid Surface Tension (N/m)	
C''_{1i}	7.040E+01
C''_{2i}	8.819E+01
C''_{3i}	-4.431E+02
C''_{4i}	9.597E+02
C''_{5i}	-7.821E+02
Liquid thermal conductivity (W/m-K)	
D_i	1.292E+01
D_{ii}	2.453E+04
D_{iii}	3.949E-08
D_{iiii}	-2.020E-09
D_{iiiii}	2.441E-12
Liquid heat Capacity (J/kmol-K)	
C'_{1i}	-2.435E+03
C'_{2i}	1.617E+05
C'_{3i}	3.380E+02

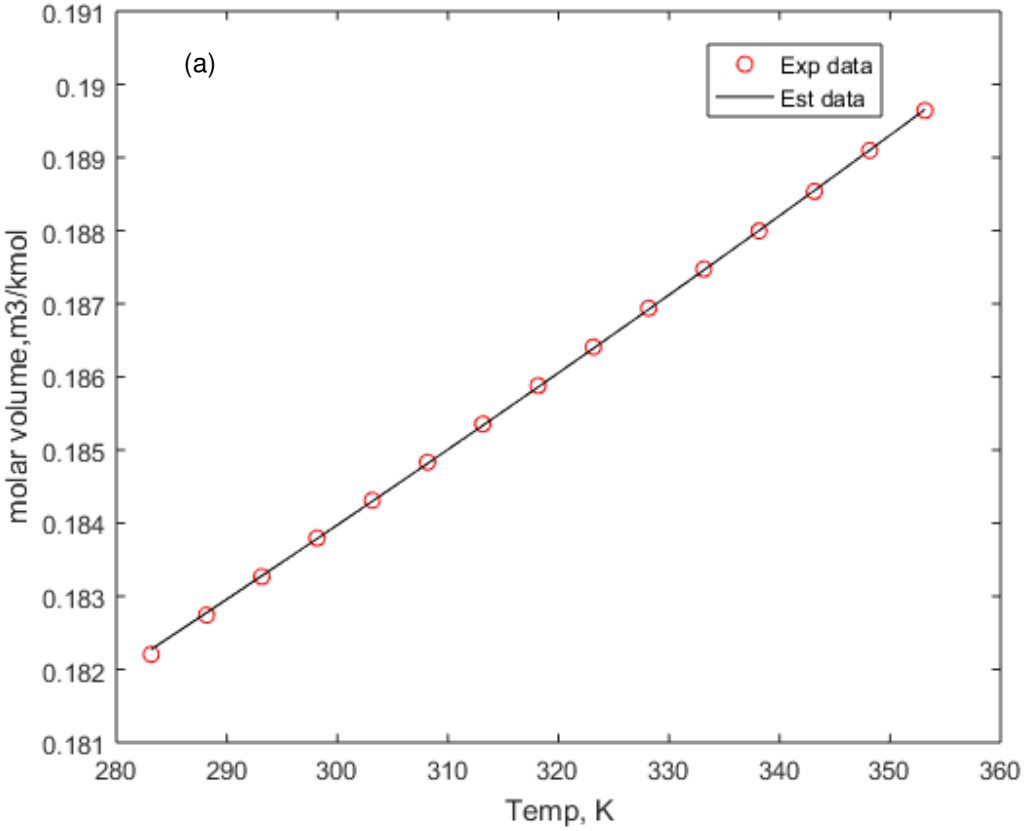
(a)
Exp data
Est data
molar volume,m3/kmol
Temp, K
0.191
0.19
0.189
0.188
0.187
0.186
0.185
0.184
0.183
0.182
0.181
280
290
300
310
320
330
340
350
360

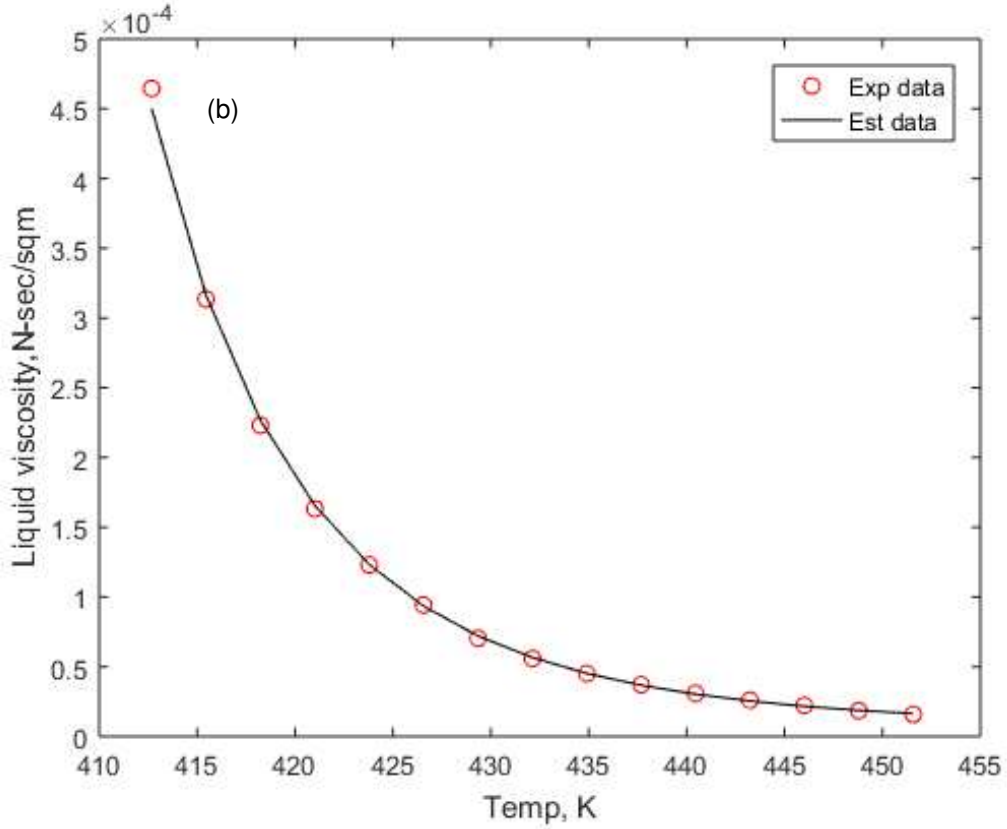
(b)
Exp data
Est data
Liquid viscosity,N-sec/sqm
Temp, K
×10^-4
5
4.5
4
3.5
3
2.5
2
1.5
1
0.5
0
410
415
420
425
430
435
440
445
450
455

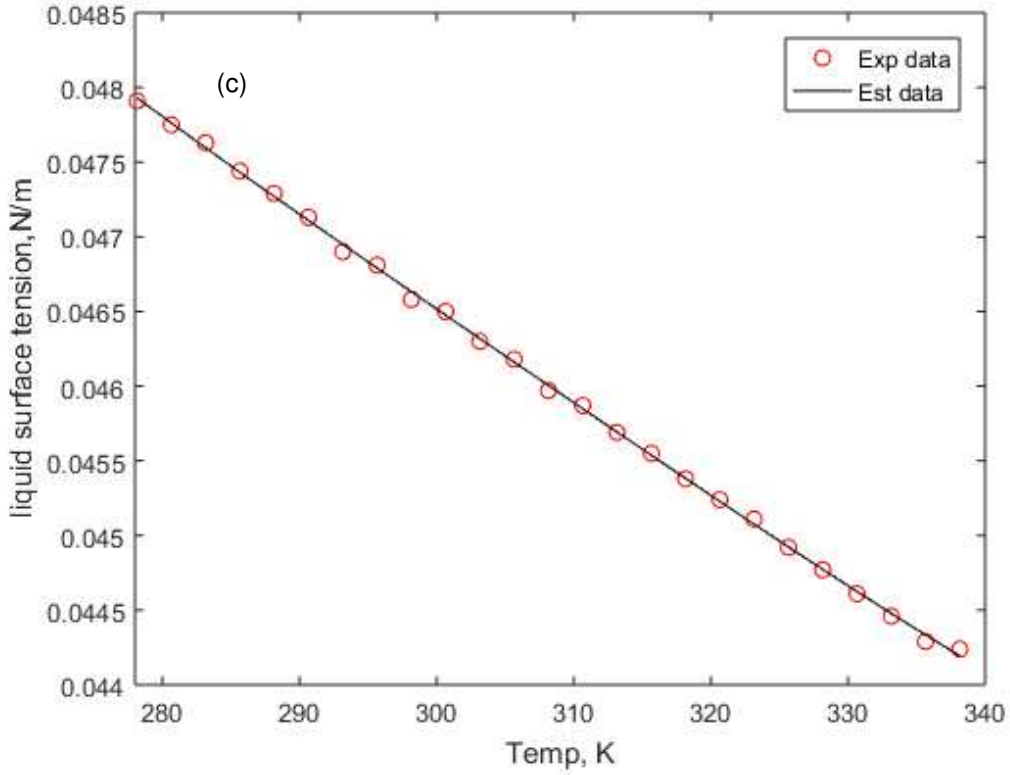
(c)
Exp data
Est data
liquid surface tension,N/m
Temp, K
0.0485
0.048
0.0475
0.047
0.0465
0.046
0.0455
0.045
0.0445
0.044
280
290
300
310
320
330
340

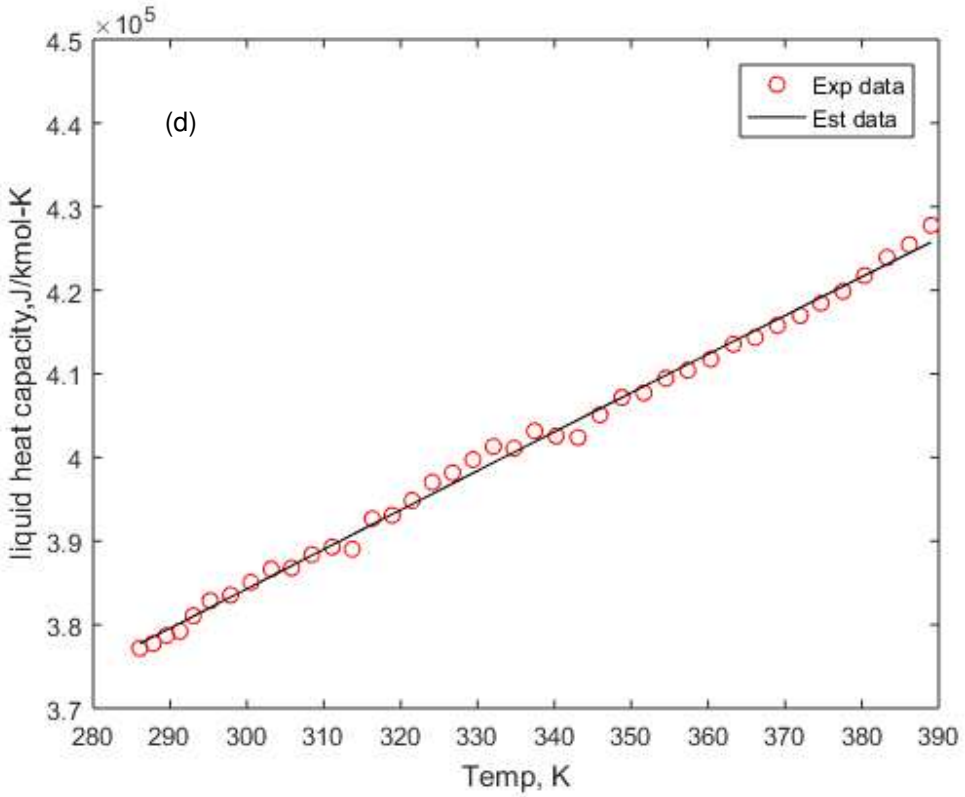
(d)
Exp data
Est data
liquid heat capacity,J/kmol-K
Temp, K
×10^5
4.5
4.4
4.3
4.2
4.1
4
3.9
3.8
3.7
280
290
300
310
320
330
340
350
360
370
380
390

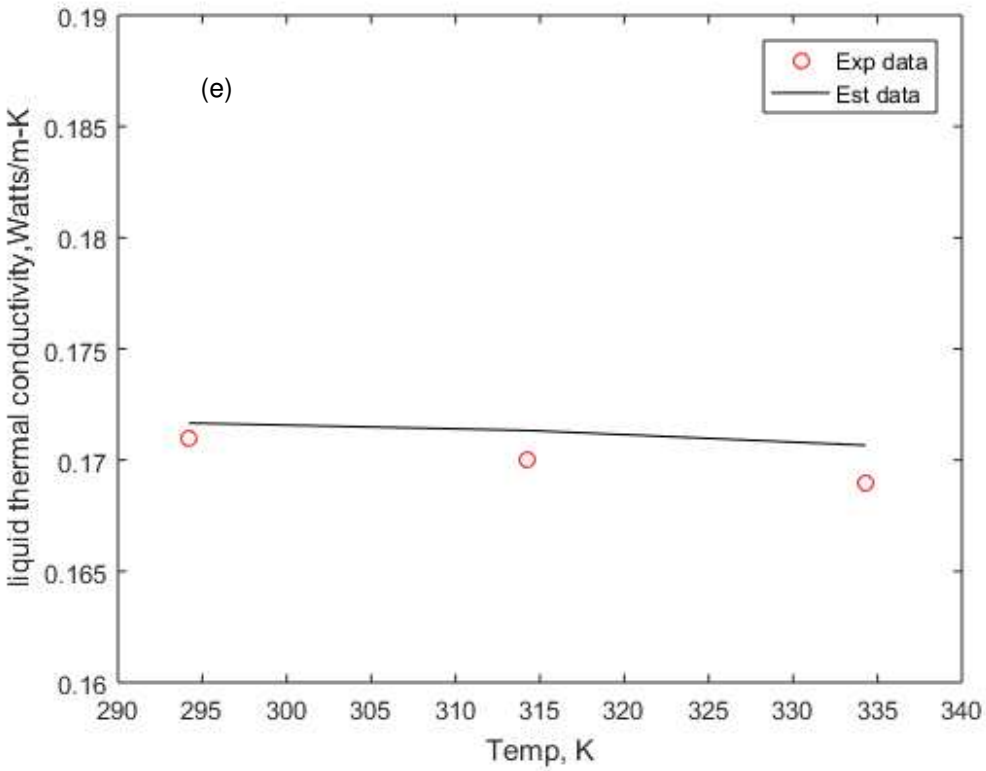

Fig. 6 Temperature dependent properties prediction for [bpy][BF_4] using Aspen Plus (a) molar volume (b) liquid viscosity (c) liquid surface tension (d) liquid heat capacity (e) liquid thermal conductivity; circles and lines denoted experimental data from literature and estimated data [13, 15, 17, 36] respectively.

5. Performance comparison of MEA and [bpy][BF_4]-MEA process

Performance evaluation of both MEA-based and [bpy][BF_4]-MEA-based process was based on the following performance index: energy performance, mass transfer within the absorber, make-up solvent required, cooling water and CO_2 removal cost. The summary of results for both process simulation is shown in Table 8.

Table 8 key parameters result summary

Process Parameters	Unit	MEA	[bpy][BF_4]-MEA
lean solvent flowrate	kg/hr	122931	129737
L/G	kg/kg	4.37	4.61
CO_2 lean loading	kmol CO_2/kmol $_{solvent}$	0.18	0.11
CO_2 Rich loading	kmol CO_2/kmol $_{solvent}$	0.59	0.42
rich solvent temperature	˚C	80	76
Reboiler temperature	˚C	120	126
Specific heat duty	GJ/tonne CO_2	4.50	3.80
Pump Duty	GJ/tonne CO_2	0.12	0.11
Cooling Water	tonne/hr	1958.59	1398.71
Make-up Solvent	kg/tonne CO_2	33.28	32.91

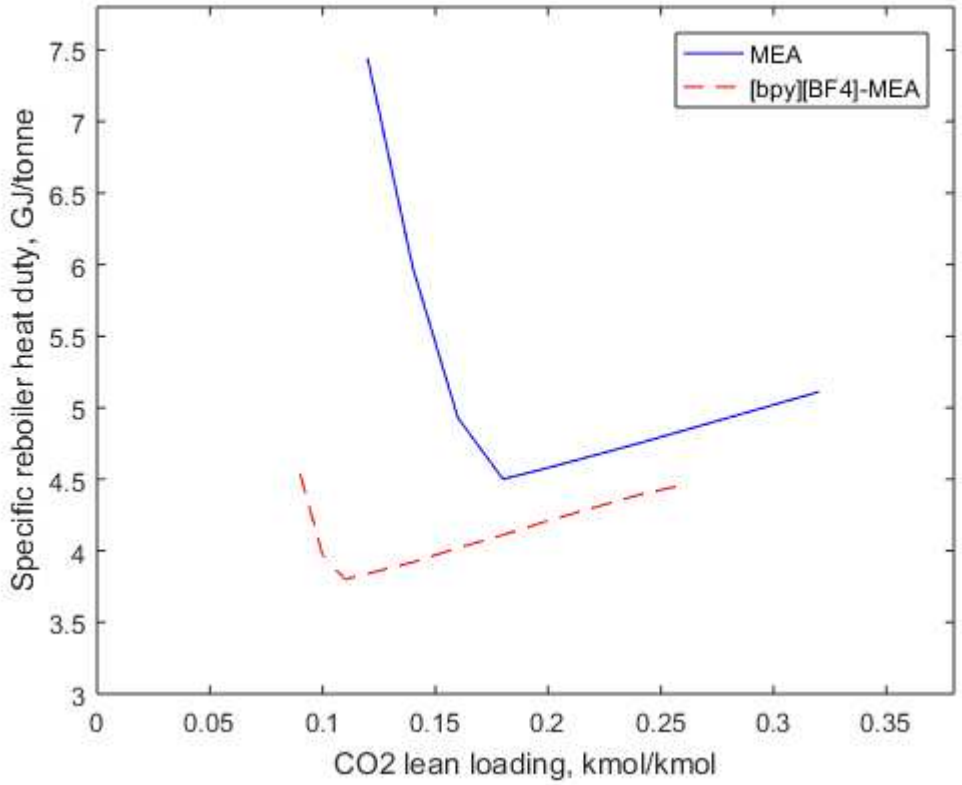

298

299 **Fig. 7 Effect of CO_2 lean loading on the specific reboiler heat duty requirement of MEA and**
300 **[bpy][BF_4]-MEA.**

301

302 5.1 Energy performance

303 The specific heat duty of MEA and [bpy][BF_4]-MEA process was evaluated by varying CO_2 lean loading
304 to achieve the minimum specific heat duty. The CO_2 loading with minimum specific heat duty for both
305 process were compared. Fig. 7 shows the specific reboiler heat duty plot as a function of CO_2 loading.
306 It can be seen that the specific heat duty decreases with increasing CO_2 loading until it gets to its
307 minimum, and then a steady rise in the specific heat duty is observed as CO_2 loading is increased
308 further. This is because at low CO_2 loading, the heat duty is mainly governed by the latent heat of
309 vaporization. The latent heat reduces as the CO_2 loading is increased until it is constant. The sensible
310 heat begins to have a dominant effect on the heat duty due to the increase in the solvent circulation
311 flowrate. The minimum specific heat duty was attained at a CO_2 loading of 0.18 for MEA process and
312 0.11 for [bpy][BF_4]-MEA based process.

313 It was observed that the specific heat duty required for [bpy][BF_4]-MEA based process (3.80GJ/tonne)
314 is less than that required for a MEA based process (4.5GJ/tonne). This is attributed to reduction of latent
315 heat and heat capacity of the hybrid solvent in a reboiler. The reduced latent heat is as a result of
316 reduced concentration of water to vaporize in the hybrid ([bpy][BF_4]-MEA) solvent. The presence of
317 [bpy][BF_4] in the hybrid solvent reduces the heat capacity despite an increase in the solvent circulation
318 flowrate.

319

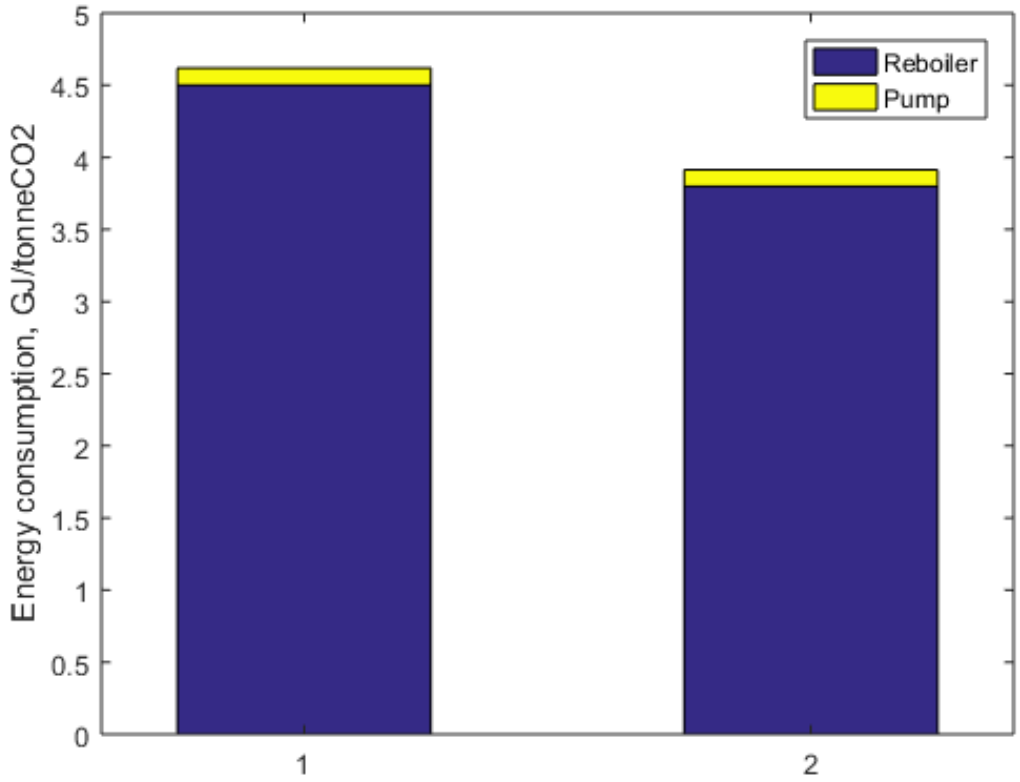

Fig. 8 Energy Consumption for MEA (1) and [bpy][BF_4]-MEA (2) based process

The energy consumption for each process is shown in Fig.8. This takes into consideration pump duty in addition to the specific heat duty. It can be seen from Fig.8 that the reboiler accounts for the largest share of energy consumed in both MEA and [bpy][BF_4]-MEA process. From Table 8, the pump duty required for the hybrid process is slightly similar compared to the MEA based process. This is because solvent circulation flowrate required for [bpy][BF_4]-MEA based process is similar compared to the MEA based process with a percentage difference of 5.54%. The [bpy][BF_4]-MEA based process is shown to be more energy saving in the reboiler by 15 % than the conventional MEA based process.

5.2 Mass Transfer

The mass transfer performance of both process was evaluated by plotting the mass transfer rate of CO_2 from the vapour phase to liquid phase in the absorber. As shown in Fig.9, both process gave a similar mass transfer performance. Despite this, it was observed from Table 8 that the solvent circulation rate for the MEA based process is slightly reduced by 5.54 % compared to the [bpy][BF_4]-MEA based process to achieve the same CO_2 removal specification. This is attributed to the high viscosity, molecular weight and density of the [bpy][BF_4]-MEA solvent compared with MEA.

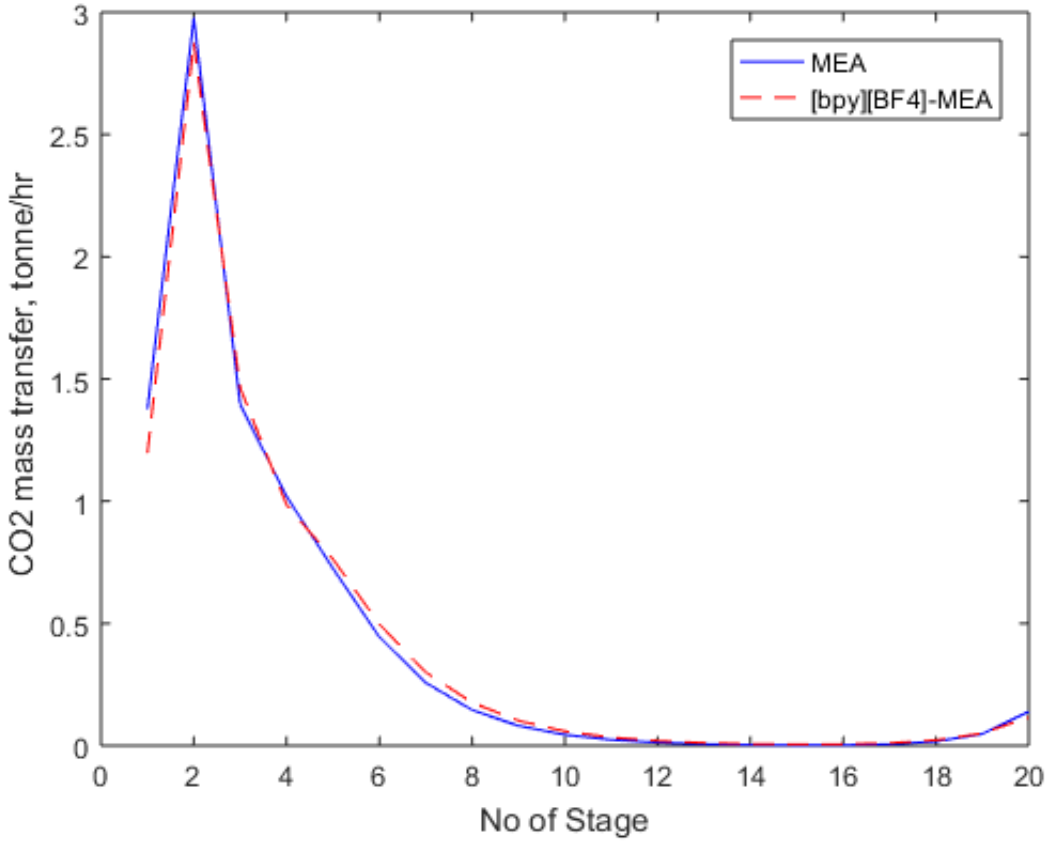

Fig. 9 CO_2 mass transfer rate (kmol/hr) in the Absorber for MEA and [bpy][BF_4]-MEA based process

5.3 Make-up Solvent

The make-up solvent is measured as the kg of solvent per tonne of CO_2 removed. From Table 8, the make-up solvent needed for the [bpy][BF_4]-MEA process is slightly lower than make-up needed for MEA process. The make-up solvent is composed of mainly MEA and H_2O. This is basically due to the low vapour pressure of [bpy][BF_4], which reduces degradation of the ionic liquid. Thus making make-up for [bpy][BF_4] negligible.

5.4 Cooling Water

The cooling water required for [bpy][BF_4]-MEA based process and MEA based process takes into consideration the cooling water required in condenser and cooler. The [bpy][BF_4]-MEA process requires less cooling water required compared with MEA process. The reduced amount of water vaporized in the stripper reduces cooling water required in the condenser duty to achieve CO_2 purity specification. The cooling water required in the cooler is reduced for the [bpy][BF_4]-MEA based process due to the increased temperature of the inlet stream to the cooler.

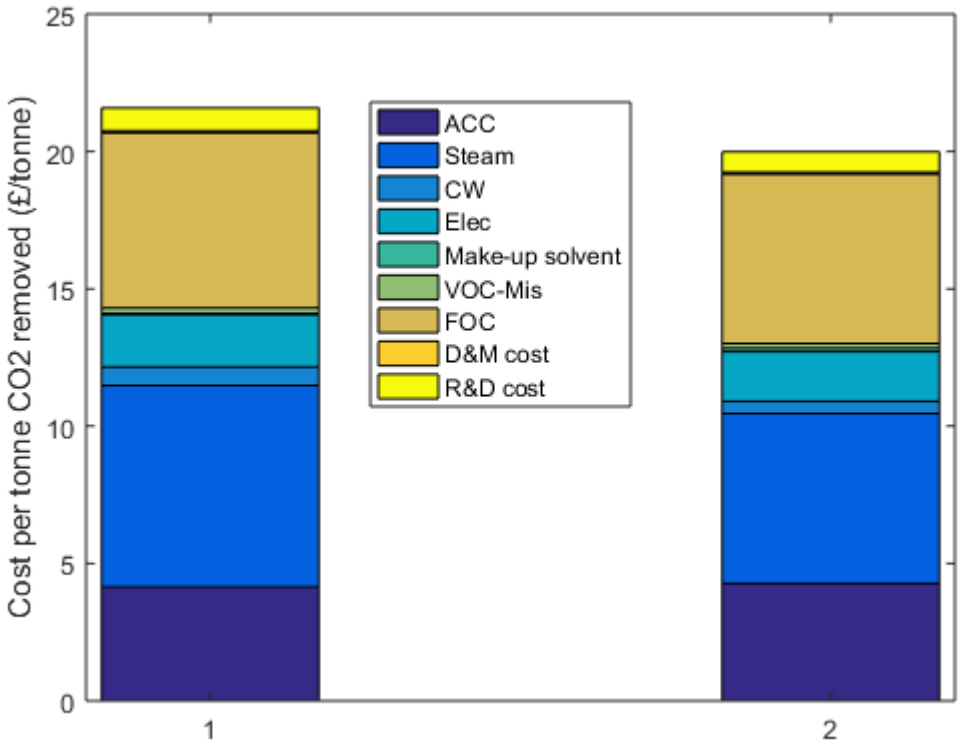

Fig. 10 Beakdown of the Cost of CO_2 removed for (1) MEA-based process and (2) [bpy][BF_4]-MEA based process

5.5 Cost Analysis

A breakdown of the cost of CO_2 removed is shown in Fig.10. This includes the annual capital cost (ACC), which is a reflection of mainly the equipment cost and initial solvent circulation cost, as well as the operating cost, which include variable operating cost (VOC) and fixed operating cost (FOC). The capital cost of the hybrid CO_2 removal process is higher than the MEA based process by 2.48%. This is due to the increase in initial solvent circulation rate and high cost of [bpy][BF_4]. It was also observed that steam cost mainly governs the process operating cost. From the study, the steam cost in the [bpy][BF_4]-MEA process was reduced by 15.55% compared with the MEA based process. Despite the increased solvent make-up cost for the [bpy][BF_4]-MEA based process, it was observed that the solvent make-up cost accounts for small percentage (0.18% and 0.67%) of the total cost of CO_2 removed for both process. The low steam cost is reflected on the reduced total cost of CO_2 removed in the [bpy][BF_4]-MEA based process (£19.98/tonne CO_2) compared with the MEA based process (£21.58/tonne CO_2). This showed an energy saving cost of £1.6/tonne CO_2 for [bpy][BF_4]-MEA based process. Based on the model result, 85,021 tonnes of CO_2 is capture annually. This implies that a savings of £136,033.06 is attained annually by adopting [bpy][BF_4]-MEA solvent, indicating that the hybrid solvent-based process is a cost-saving system. See Table 9 for details on the cost of CO_2 removed.

Table 9 Beakdown of the Cost of CO_2 removed for (1) MEA-based process and (2) [bpy][BF_4]-MEA based process

Cost	MEA –based process (£/CO_2 removed)	[bpy][BF_4]-MEA based process (£/CO_2 removed)
ACC	4.15	4.25
VOC steam	7.33	6.19
VOC water	0.67	0.45
VOC electricity	1.91	1.80
Make -up Solvent	0.04	0.13
VOC Miscellaneous	0.20	0.17
FOC	6.37	6.15
Distribution & market	0.08	0.07
R&D cost	0.83	0.75
Total	21.58	19.98

6. Effect of [bpy][BF_4] Concentration

Fig. 11 shows a plot on the effect of [bpy][BF_4] Concentration on the L/G ratio of the absorber and reboiler heat duty. The L/G ratio and specific heat duty reflects the solvent circulation rate and the reboiler steam rate required to meet CO_2 removal specifications. The concentration of [bpy][BF_4] in the hybrid solvent was varied 0wt% to 35wt%. 0wt% of [bpy][BF_4] represents the MEA based process. It was observed that an introduction of a small concentration (5wt%) of [bpy][BF_4] slightly reduces the L/G ratio but a further [bpy][BF_4] concentration increase resulted to relatively steady rise in the L/G ratio. Also, the specific reboiler heat duty reduces as the concentration of [bpy][BF_4] is increased. This indicates that less amount of steam, which basically governs the CO_2 removal cost, is required in the reboiler to meet the CO_2 removal specification with increasing [bpy][BF_4] concentration . This is attributed to decreasing heat capacity of the hybrid solvent as with the presence of [bpy][BF_4] in hybrid solvent.

The plot in Fig. 12 shows the cost of CO_2 removed (as annual capital (ACC) and annual operating cost (AOC)) as a function of the concentration of [bpy][BF_4]. This is to investigate the concentration of [bpy][BF_4] required in the hybrid solvent to achieve the minimum cost of CO_2 removed. From Fig. 12, The minimum cost of CO_2 removed (£19.98/tonne CO_2) was attained at 30wt% of [bpy][BF_4]. This is due to the reduced annual operating cost despite the increase in annual capital cost. It can be seen from Fig. 12 that after 30wt% of [bpy][BF_4], the cost of CO_2 removed increases. This implies that the significance of capital cost to the cost of CO_2 removed increases because of the initial solvent cost increased despite the reduced operating cost.

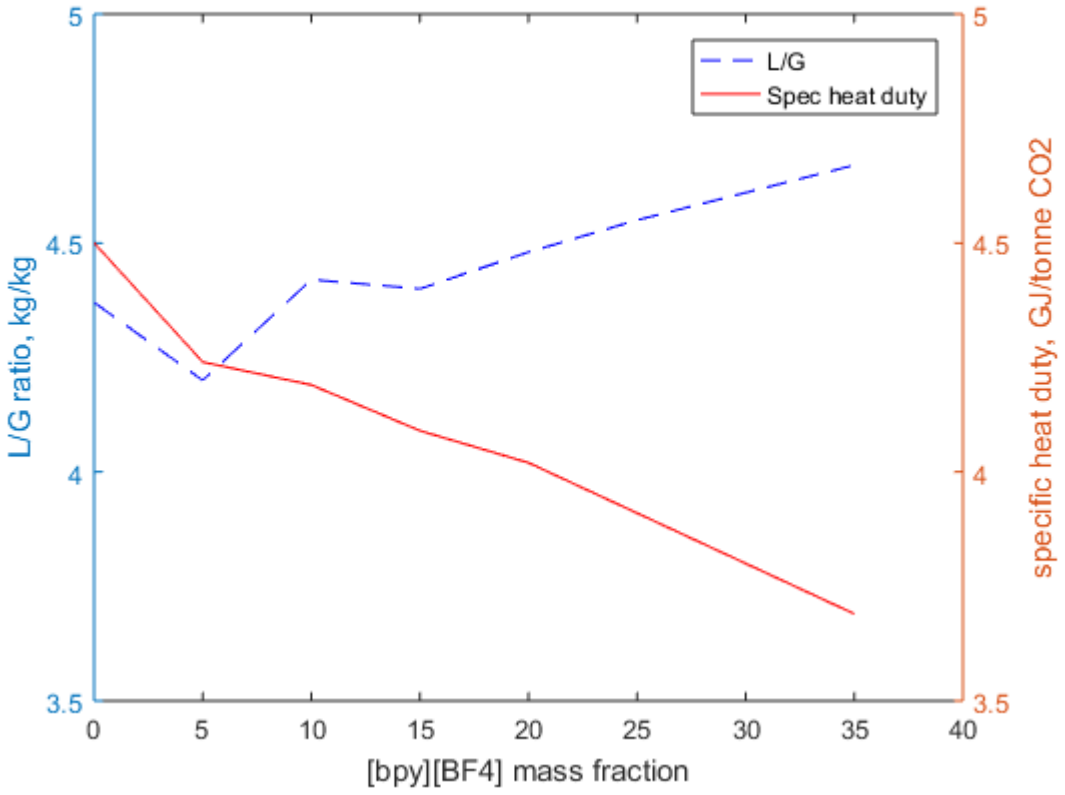

397

398 **Fig. 11 Effect of [bpy][BF_4] mass fraction on L/G (kg/kg) (dashed line) and Specific heat duty**
399 **(GJ/tonne CO_2) (straight line) in the [bpy][BF_4]-MEA based process.**

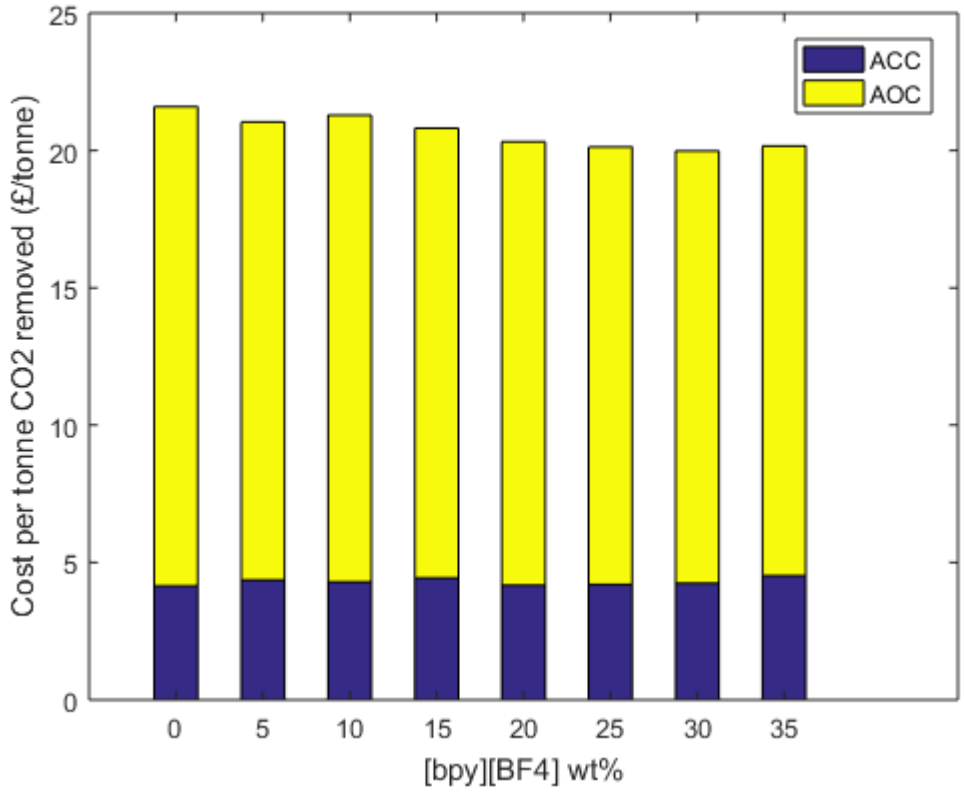

400

401 **Fig. 12 Effect of [bpy][BF_4] mass percentage on the Cost of CO_2 removed**

7. Conclusion

Application of IL-MEA process for CO_2 capture from power plant flue gases has been [11]. Similar investigation has not been performed for CO_2 removal process in natural gas cleaning in operations. This study aims to fill the gap by providing a comparative study of conventional MEA and IL-MEA based process for natural gas sweetening through modelling and simulation. This study assesses the process and energy performance of the hybrid (IL-MEA) solvent, which can replace the conventional amine as the future solvent.

The physiochemical properties of IL ([bpy][BF_4]) used in this study were estimated using Aspen Plus®. The results were shown to agree well with the experimental data from literature. The [bpy][BF_4]-MEA based process with lean solvent composition of 30wt% MEA, 30wt% [bpy][BF_4] and 40.0wt% H_2O showed an energy savings of 15% in the reboiler duty and a reduction of 7.44% in the cost of CO_2 avoidance compared to the MEA (30wt%) based process. Despite the reduced solvent circulation rate in the MEA based process and high cost of [bpy][BF_4], the hybrid solvent-based process proved to be more cost efficient. This is due to the reduced operating cost of the [bpy][BF_4]-MEA based process as result of the low utilities (majorly steam) cost. Further analysis on the effect of [bpy][BF_4] concentration on the process performance and cost of CO_2 removed was carried out. An increase in the concentration of [bpy][BF_4] resulted in a rise in L/G ratio (solvent circulation rate) and a reduction in the overall energy consumption. Also, the cost of CO_2 removed is reduced with increasing [bpy][BF_4] concentration. From the economic analysis, the 30wt% concentration of [bpy][BF_4] in the [bpy][BF_4]-MEA based process achieved the minimal cost of CO_2 removed. Thus, [bpy][BF_4]-MEA based solvent was able to achieve an energy and cost-efficient capture process.

References

[1] Sims REH, Rogner H-H, Gregory K. Carbon emission and mitigation cost comparisons between fossil fuel, nuclear and renewable energy resources for electricity generation. Energy Policy 2003;31(13):1315-26.

[2] Huaman RNE, Jun TX. Energy related CO_2 emissions and the progress on CCS projects: a review. Renewable and Sustainable Energy Reviews 2014;31:368-85.

[3] Rufford TE, Smart S, Watson GCY, Graham BF, Boxall J, da Costa JCD, et al. The removal of CO_2 and N_2 from natural gas: a review of conventional and emerging process technologies. Journal of Petroleum Science and Engineering 2012;94:123-54.

[4] Burgers WFJ, Northrop PS, Kheshgi HS, Valencia JA. Worldwide development potential for sour gas. Energy Procedia 2011;4:2178-84.

[5] Kumar S, Cho JH, Moon I. Ionic liquid-amine blends and CO_2 BOLs: prospective solvents for natural gas sweetening and CO_2 capture technology—a review. International Journal of Greenhouse Gas Control 2014;20:87-116.

[6] Kidnay AJ, Parrish WR, McCartney DG. Fundamentals of natural gas processing. CRC Press; 2011.

[7] Liu X, Chen J, Luo X, Wang M, Meng H. Study on heat integration of supercritical coal-fired power plant with post-combustion CO_2 capture process through process simulation. Fuel 2015;158:625–33.

[8] Olajire AA. CO_2 capture and separation technologies for end-of-pipe applications–a review. Energy 2010;35(6):2610-28.

[9] Kohl AL, Nielsen R. Gas purification. Gulf Professional Publishing; 1997.

[10] Das D, Meikap BC. Comparison of adsorption capacity of mono-ethanolamine and di-ethanolamine impregnated activated carbon in a multi-staged fluidized bed reactor for carbon-dioxide capture. Fuel 2018;224:47–56

[11] Huang Y, Zhang X, Zhang X, Dong H, Zhang S. Thermodynamic modeling and assessment of ionic liquid-based CO_2 capture processes. Industrial & Engineering Chemistry Research 2014;53(29):11805-17.

[12] Cadena C, Anthony JL, Shah JK, Morrow TI, Brennecke JF, Maginn EJ. Why is CO_2 so Soluble in Imidazolium-Based Ionic Liquids? Journal of the American Chemical Society 2004;126(16):5300-8.

[13] Bandrés I, Royo FM, Gascón I, Castro M, Lafuente C. Anion influence on thermophysical properties of ionic liquids: 1-butylpyridinium tetrafluoroborate and 1-butylpyridinium triflate. The Journal of Physical Chemistry B 2010;114(10):3601-7.

[14] Llovell F, Marcos RM, MacDowell N, Vega LF. Modeling the absorption of weak electrolytes and acid gases with ionic liquids using the soft-SAFT approach. Journal of Physical Chemistry B 2012;116(26):7709-18.

[15] Mokhtarani B, Sharifi A, Mortaheb HR, Mirzaei M, Mafi M, Sadeghian F. Density and viscosity of pyridinium-based ionic liquids and their binary mixtures with water at several temperatures. The Journal of Chemical Thermodynamics 2009;41(3):323-9.

[16] Supasitmongkol S, Styring P. High CO_2 solubility in ionic liquids and a tetraalkylammonium-based poly(ionic liquid). Energy and Environmental Science 2010;3(12):1961-72.

[17] Tomida D, Kenmochi S, Qiao K, Tsukada T, Yokoyama C. Densities and thermal conductivities of N-alkylpyridinium tetrafluoroborates at high pressure. Fluid Phase Equilibria 2013;340:31-6.

[18] Torralba-Calleja E, Skinner J, Gutiérrez-Tauste D. CO_2 capture in ionic liquids: A review of solubilities and experimental methods. Journal of Chemistry 2013.

[19] Yunus NM, Mutalib MIA, Man Z, Bustam MA, Murugesan T. Solubility of CO_2 in pyridinium based ionic liquids. Chemical Engineering Journal 2012;189:94-100.

[20] Camper D, Bara JE, Gin DL, Noble RD. Room-temperature ionic liquid− amine solutions: Tunable solvents for efficient and reversible capture of CO_2. Industrial & Engineering Chemistry Research 2008;47(21):8496-8.

[21] Feng Z, Cheng-Gang F, You-Ting W, Yuan-Tao W, Ai-Min L, Zhi-Bing Z. Absorption of CO_2 in the aqueous solutions of functionalized ionic liquids and MDEA. Chemical Engineering Journal 2010;160(2):691-7.

[22] Taib MM, Murugesan T. Solubilities of CO_2 in aqueous solutions of ionic liquids (ILs) and monoethanolamine (MEA) at pressures from 100 to 1600kPa. Chemical Engineering Journal 2012;181-182:56-62.

[23] Zhao Y, Zhang X, Dong H, Zhen Y, Li G, Zeng S, et al. Solubilities of gases in novel alcamines ionic liquid 2-[2-hydroxyethyl (methyl) amino] ethanol chloride. Fluid Phase Equilibria 2011;302(1):60-4.

[24] Baj S, Siewniak A, Chrobok A, Krawczyk T, Sobolewski A. Monoethanolamine and ionic liquid aqueous solutions as effective systems for CO_2 capture. Journal of Chemical Technology and Biotechnology 2013;88(7):1220-7.

[25] Zhao Y, Zhang X, Zeng S, Zhou Q, Dong H, Tian X, et al. Density, viscosity, and performances of carbon dioxide capture in 16 absorbents of amine ionic liquid H_2O, ionic liquid H_2O, and amine H_2O systems. Journal of Chemical & Engineering Data 2010;55(9):3513-9.

[26] Yang J, Yu X, Yan J, Tu S-T. CO2 capture using amine solution mixed with ionic liquid. Industrial & Engineering Chemistry Research 2014;53(7):2790-9.

[27] Hasib-Ur-Rahman M, Bouteldja H, Fongarland P, Siaj M, Larachi F. Corrosion behavior of carbon steel in alkanolamine/room-temperature ionic liquid based CO_2 capture systems. Industrial and Engineering Chemistry Research 2012;51(26):8711-8.

[28] Khan SN, Hailegiorgis SM, Man Z, Garg S, Shariff AM, Farrukh S, et al. High-pressure absorption study of CO_2 in aqueous N-methyldiethanolamine (MDEA) and MDEA-piperazine (PZ)-1-butyl-3-methylimidazolium trifluoromethanesulfonate [bmim][OTf] hybrid solvents. Journal of Molecular Liquids 2018;249:1236-44.

[29] Khan SN, Hailegiorgis SM, Man Z, Shariff AM, Garg S. Thermophysical properties of aqueous N-methyldiethanolamine (MDEA) and ionic liquids 1-butyl-3-methylimidazolium trifluoromethanesulfonate [bmim][OTf], 1-butyl-3-methylimidazolium acetate [bmim][Ac] hybrid solvents for CO_2 capture. Chemical Engineering Research and Design 2017;121:69-80.

[30] Hailegiorgis SM, Khan SN, Abdolah NHH, Ayoub M, Tesfamichael A. Carbon dioxide capture via aqueous N-methyldiethanolamine (MDEA)-1-butyl-3-methylimidazolium acetate ([bmim][Ac]) hybrid solvent. *AIP Conference Proceedings*. 1891. 2017.

[31] Zoubeik M, Mohamedali M, Henni A. Experimental solubility and thermodynamic modeling of CO_2 in four new imidazolium and pyridinium-based ionic liquids. Fluid Phase Equilib 2016;419:67–74.

[32] Huang Y, Dong H, Zhang X, Li C, Zhang S. A new fragment contribution-corresponding states method for physicochemical properties prediction of ionic liquids. AIChE Journal 2013;59(4):1348-59.

[33] Zacchello B, Oko E, Wang M, Fethi A. Process simulation and analysis of carbon capture with an aqueous mixture of ionic liquid and monoethanolamine solvent. International Journal of Coal Science & Technology 2017;4(1):25-32.

[34] Oko E, Zacchello B, Wang M, Fethi A. Process analysis and economic evaluation of mixed aqueous ionic liquid and monoethanolamine (MEA) solvent for CO_2 capture from a coke oven plant. Greenhouse Gases: Science and Technology 2018;1-15.doi:10.1002/ghg.1772.

[35] Couling DJ, Bernot RJ, Docherty KM, Dixon JK, Maginn EJ. Assessing the factors responsible for ionic liquid toxicity to aquatic organisms via quantitative structure–property relationship modeling. Green Chemistry 2006;8(1):82-90.

[36] Zhang ZH, Tan ZC, Li YS, Sun LX. Thermodynamic investigation of room temperature ionic liquid. Journal of thermal analysis and calorimetry 2006;85(3):551-7.

[37] Younger AH. Natural Gas Processing Principles and Technology-part 2. Gas Processors Association, Tulsa Oklahoma 2004.

[38] Gpsa G. Engineering data book. Gas Processors Suppliers Association 2004;2:16-24.

[39] Lawal A, Wang M, Stephenson P, Koumpouras G, Yeung H. Dynamic modelling and analysis of post-combustion CO_2 chemical absorption process for coal-fired power plants. Fuel 2010;89(10):2791-801.

[40] Aspen HYSYS. Tutorials and Applications. Aspen Technology. Inc, Burlington, Massachusetts,USA 2007.

[41] Chattopadhyay P. Absorption & Stripping. Asian Books Private Limited; 2007.

[42] Lin Y-J, Pan T-H, Wong DS-H, Jang S-S, Chi Y-W, Yeh C-H. Plantwide control of CO_2 capture by absorption and stripping using monoethanolamine solution. Industrial & Engineering Chemistry Research 2010;50(3):1338-45.

[43] Jacquemin J, Gomes MFC, Husson P, Majer V. Solubility of carbon dioxide, ethane, methane, oxygen, nitrogen, hydrogen, argon, and carbon monoxide in 1-butyl-3-methylimidazolium tetrafluoroborate between temperatures 283K and 343K and at pressures close to atmospheric. The Journal of Chemical Thermodynamics 2006;38(4):490-502.

[44] Bravo JL, Rocha JA, Fair JR. Mass transfer in gauze packings. Hydrocarbon Processing 1985;64(1):91-5.

[45] Karimi M, Hillestad M, Svendsen HF. Capital costs and energy considerations of different alternative stripper configurations for post combustion CO_2 capture. Chemical Engineering Research and Design 2011;89(8):1229-36.

543 [46] Mores P, Rodríguez N, Scenna N, Mussati S. CO_2 capture in power plants: Minimization of the
544 investment and operating cost of the post-combustion process using MEA aqueous solution.
545 International Journal of Greenhouse Gas Control 2012;10(Supplement C):148-63.